Indian Journal of Biochemistry & Biophysics
Vol. 60, September 2023, pp. 729-740
DOI: 10.56042/ijbb.v60i9.3877

Synthesis, DFT and Molecular docking study of novel bis 1,2,3-triazole derivatives of 2-hydroxyquinoline-4-carboxylate as antimicrobial agents

Kandukuri Usha Rani[1], Gangavaram VM Sharma[2], Shalini Saxena[3], Lalitha Guruprasad[3] & DA Padmavathi[1]*

[1]Department of Chemistry, University College of Science, Osmania University, Hyderabad- 500 007, Telangana, India
[2]Organic and Bimolecular Chemistry Division, CSIR-Indian Institute of Chemical Technology, Hyderabad-500 007, Telangana, India
[3]School of Chemistry, University of Hyderabad, Hyderabad-500 046, Telangana, India

Received 28 June 2023; *revised 05 August 2023*

A series of novel bis 1,2,3-triazole derivatives of 2-Hydroxyquinoline-4-carboxylate, exhibiting diverse molecular structures were synthesized through a click reaction, incorporating a combination of 1,2,3-triazole moieties and quinoline nucleus. *In vitro* biological studies were conducted to evaluate their antitubercular, antibacterial and antifungal activities. To explore the behavioural and selective properties of the synthesized molecules, experimental analysis was complemented with computational methods. Density functional theory (DFT) calculations were performed to examine electronic and structural parameters, while molecular docking studies were conducted to gain insight into the structural basis of activity against MTB InhA inhibitors, DNA gyrase B protein of *Staphylococcus aureus* (a Gram positive bacterium) and DHFR of *Candida albicans* fungi. Theoretical calculations were consistent with the observed antibacterial and antifungal activity in the experimental data.

Keywords: 1,2,3-triazoles, Antimicrobial activity, DFT, Molecular docking, Quinolines

Triazoles and their derivatives are important in medicinal chemistry and are used for synthesising variable heterocyclics with different biological activities. 1,2,3-triazoles have been of great interest due to their useful applications as chemotherapeutic agents. The 1,2,3-triazole system[1] is highly stable due to aromaticity, and also due to the presence of both acidic and basic nitrogen's in the same moiety. These nitrogen heterocycles due to their high dipole moments interact with biomolecular targets through dipolar interactions. Triazoles exhibit a wide range of biological activities[2] including antimicrobial[3], antiviral[4], anti-inflammatory, analgesic[5], anticancer[6], antifungal (Manclús *et al*. 2008)[7] and anticonvulsant[8] effects. These diverse activities render triazoles valuable in therapeutic applications.

Quinoline, a highly promising heterocyclic nucleus, present in both natural and synthesized molecules, holds immense therapeutic significance. This pharmacophore is adept at producing compounds that exhibit a wide range of activities including anticancer, antimicrobial, antimalarial, anti-inflammatory, neuroprotective, and antiviral effects[9]. Derivatives derived from quinoline not only possess significant medicinal value but have also demonstrated success as effective pharmaceuticals. The urea derivative of quinoline lenvatinib, is used for thyroid cancer treatment, and topotecan is used to treat ovarian, cervical and lung cancers. And, Chloroquine is the well-known drug to treat malaria. Recently, bedaquiline is approved for the treatment of multi-drug resistant tuberculosis[9]. Some other antibiotics with fluoroquinolone skeleton ex., Gatifloxacin, Moxifloxacin and Levofloxacin, exhibit excellent bactericidal activity[10-12]. Some novel N-(8-hydroxyQuinoline-5-yl)-aminoglyoximes have antibacterial activities and antifungal activities. So to develop new anti-microbial drugs one can plan with variable and multiple substituents on quinoline moiety[13].

Taking into account the antitubercular and antimicrobial efficacy, along with the lipophilicity of substituent groups that can impact the bioactivity of quinolines, a series of bis 1,2,3-triazole derivatives of 2-hydroxyquinoline-4-carboxylate were formulated and synthesized. These derivatives encompass a blend of quinolines and substituted 1,2,3-triazoles. *In vitro* studies investigations were carried out to evaluate the antitubercular[14] and antimicrobial[15] activities of the ten synthesized quinoline derivatives.

*Correspondence:
E-mail: dapadma@rediffmail.com
Suppl. Data available on respective page of NOPR

This paper explores the impact of combining these two potent pharmacophores on the antibacterial and antifungal activities of the designed molecules.

Results and Discussion

The structures of the synthesized compounds have been established on the basis of spectral data from ^{1}HNMR, HRMS, and IR techniques. The ^{1}HNMR spectra were recorded using a Bruker AVANCE III-500 MHz spectrometer at temperatures ranging from 278-303 K, in $CDCl_3$ and DMSO-d_6 solvents. Tetramethyl silane (TMS) was used as an internal standard for referencing the chemical shifts, which are expressed in δ scales. All chemical shifts and coupling constants were determined from the ^{1}H NMR spectra. High-resolution mass spectra HRMS were acquired using a Q-TOF (Agilent) mass spectrometer.

Prop-2-yn-1-yl2-(prop-2-yn-1-yloxy)quinoline-4-carboxylate (compound 2) was synthesized from 2-hydroxyquinoline-4-carboxylic acid (compound 1) with propargyl bromide. The reaction involved treating compound 1 with propargyl bromide and K_2CO_3 in dimethyl formamide DMF at normal room temperature for 4 h. The reaction yielded the desired ester 2 (quinoline di acetylene) with a yield of 80% (Scheme 1).

The ^{1}H proton NMR resonances of 2 unveiled their appearance at δ 2.51, 2.27 as a single corresponding to acetylenic proton, while the aromatic protons resonated at δ 8.37, 7.58, 7.34 as doublets and δ 7.67 as multiplet. Proton 3 of quinoline moiety resonated at 7.27 as singlet. The propargylic protons appeared at δ5.13, 4.99 as a doublet. All chemical shift values of remaining protons appeared as predicted. Furthermore, the HRMS(M+H)$^+$ peak at *m/z* 266.0806 authenticate the assigned structure 2 (Scheme 1). Different azides 3.1-3.10 (Table 1), were prepared successfully by a two-step sequence[14].

Then using click chemistry, the prepared diverse azides 3.1-3.10 on reaction with quinoline di acetylene 2 in the presence of copper(II) sulphate pentahydrate and sodium ascorbate in aq. t-BuOH (1:1) at room temperature for 8 h afforded the triazole 4.1-4.10 (Scheme 2). Using the procedure outlined in Scheme 2, all the ten distinct bis 1,2,3-triazole derivatives of 2-Hydroxyquinoline-4-carboxylate were synthesized. The synthesised carboxylate compounds along with their corresponding yields, are provided in (Scheme 2).

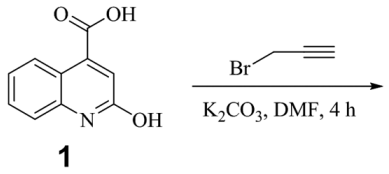

Scheme 1

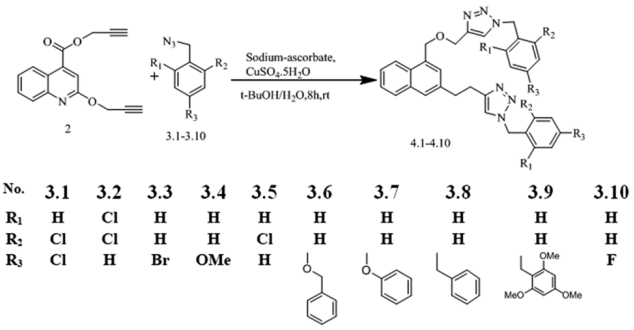

Scheme 2

Table 1 — List of diverse azides 3.1-3.10

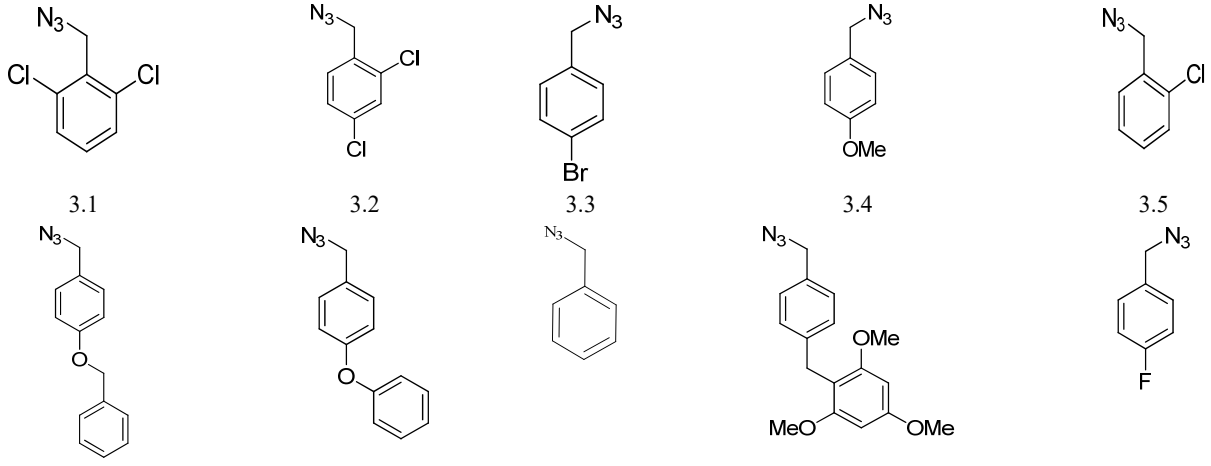

Experimental section

Prop-2-yn-1-yl 2-(prop-2-yn-1-yloxy) quinoline-4-carboxylate (2)

To a solution of 1 (4.0 g, 21.16 mmol) in dry DMF (20 mL) cooled to (0°C), K_2CO_3 (8.76 g, 63.49 mmol) was added and stirred for 30 min. Then, propargyl bromide solution (5.54 g, 46.56 mmol) was added and stirred at 23°C for 6 h. Later, the reaction mixture was treated with aq. NH_4Cl (10 mL) and extracted with EtOAc (2 × 50 mL). The combined organic layers were washed with water (2 × 30 mL), brine (50 mL) and dried (Na_2SO_4). Solvent was made to evaporate under reduced pressure and the residue is purified using column chromatography (60-120 mesh Silica gel, 8% ethyl acetate in pet. ether) to give 2 (4.5 g, 80.35%) a light yellow solid. ^{1}H NMR (500 MHz, $CDCl_3$): δ 8.37 (dd, 1H, *J* = 8.2, 1.3 Hz), 7.67 (ddd, 1H, *J* = 8.6, 7.2, 1.4 Hz), 7.58 (d, 1H,*J* = 8.1 Hz), 7.34 (ddd, 1H,*J* = 8.2, 7.2, 1.0 Hz), 7.27 (s, 1H), 5.13 (d,2H, *J* = 2.3 Hz), 4.99 (d, 2H, *J* = 2.5 Hz), 2.58 (s,), 2.27 (s, 1H). HRMS (ESI+): *m/z* $(M+H)^+$ calculated for $C_{16}H_{12}O_3N$ 266.0812, is found as 266.0806.

(1-(2,4-dichlorobenzyl)-1H-1,2,3-triazol-4-yl)methyl2-((1-(2,4-dichlorobenzyl)-1H-1,2,3triazol-4-yl)methoxy)quinoline-4-carboxylate(4.1)

A mixture of azide 3.1(0.20 g, 0.99 mmol) and quinoline di acetylene 2(0.264 g, 0.99 mmol) was dissolved in 1 mL of t-BuOH and 1 mL of water. To this solution, the sodium salt of ascorbic acid ($C_6H_7O_6Na$) (0.1 g, 0.49 mmol) was added. Subsequently, copper sulphate pentahydrate (12.3 × 10^{-3} g, 0.05 mmol) was introduced at a temperature of 25°C, and the reaction mixture was stirred for a duration of 8 h. Then, the solvent was removed by evaporating the reaction mixture. Later, the residue was diluted with 5 mL of water and extracted with 20 mL of ethyl acetate (EtOAc) and the combined organic layers were washed with 5 mL of brine and dried with sodium sulphate (Na_2SO_4). Then after evaporating the solvent, the residue was purified using chromatographic column (Silica gel: 60-120 mesh and15% ethyl acetatein pet. Ether) to afford 4.1 (0.45 g, 68%) as a light yellow solid; IR ($CHCl_3$): 3204, 3076, 1804, 1788, 1644, 1548, 1516, 1372, 1308, 1260, 1252 cm^{-1}; ^{1}H NMR (500 MHz, $CDCl_3$): δ 8.24 (dd, 1H, *J* = 8.2, 1.3 Hz), 7.96 (d,1H, *J* = 8.5 Hz), 7.67 – 7.58 (m, 2H), 7.55 (s, 1H), 7.36 – 7.27 (m, 4H), 7.22 (s, 1H), 7.19 – 7.14 (m, 2H), 7.10 (d, 1H, *J* = 7.3 Hz), 5.56 (s, 2H), 5.52 (s, 2H), 5.51 (s, 2H), 5.40 (s, 2H). HRMS (ESI+): *m/z* $(M+H)^+$ calculated for $C_{30}H_{22}Cl_4N_7O_3$ 670.0499, found 670.0491.

(1-(2,6-dichlorobenzyl)-1H-1,2,3-triazol-4-yl)methyl2-((1-(2,6-dichlorobenzyl)-1H-1,2,3-triazol-4-yl)methoxy)quinoline-4-carboxylate (4.2)

Though the preparation of 4.2 from 3.2 is similar to 4.1, the difference lies in purifying the residue through chromatographic column (Silica gel: 60-120 mesh and90% EtOAc in pet. Ether)to afford 4.2(0.34 g, 51%) as a white solid; IR ($CHCl_3$): 3204, 3076, 1804, 1788, 1644, 1548, 1516, 1372,1308, 1260, 1252 cm^{-1}; ^{1}H NMR (500 MHz, $CDCl_3$): δ 8.21 (d,1H, *J* = 7.2 Hz),8.00 (d, 1H,*J* = 8.1 Hz), 7.66 (s, 1H),), 7.64 – 7.52 (m, 2H),7.47 – 7.31 (m, 4H), 7.28 (d, 2H, *J* = 10.3 Hz), 5.89 (s, 2H), 5.78 (s, 2H), 5.54 (s, 2H), 5.49 (s, 2H). HRMS (ESI+): *m/z* $(M+H)^+$ calculated for $C_{30}H_{22}Cl_4N_7O_3$ 670.0499, found 670.0491.

(1-(4-bromobenzyl)-1H-1,2,3-triazol-4-yl)methyl2-((1-(4-bromobenzyl)-1H-1,2,3-triazol-4-yl)methoxy) quinoline-4-carboxylate (4.3)

A solution of azide 3.3 (0.20 g, 0.94 mmol) and quinoline di acetylene 2(0.25 g, 0.94 × 10^{-3} mol) taken in 1 mL of t-BuOH and 1 mL of water was treated with sodium salt of ascorbic acid ($C_6H_7O_6Na$) (94 × 10^{-3} g, 0.47 mmol). This was followed by addition of copper sulphate pentahydrate (11.85 × 10^{-3} g, 0.047 mmol) at 25°C temperature and stirred for a duration of 8 h. The reaction mixture was evaporated to remove the solvent. Later, the residue was diluted with 5 mL of water and extracted with 20 mL of EtOAc and the combined organic layers were washed with 5 mL of brine and dried with sodium sulphate (Na_2SO_4). Then after evaporating the solvent, the residue was purified using column chromatography (Silica gel: 60-120 mesh and 65% of ethyl acetate (EtOAc) in pet. Ether) to afford 4.3 (0.28 g, 42%) as a white solid; IR ($CHCl_3$): 3204, 3092, 3084, 1804, 1644, 1540,1364, 1260 cm^{-1}; ^{1}H NMR (500 MHz, $CDCl_3$): δ 8.23 (dd, 1H, *J* = 8.2, 1.3 Hz), 7.96 (d, 1H, *J* = 8.5 Hz), 7.64 – 7.61 (m, 1H), 7.61 (s, 1H), 7.54 (s, 1H), 7.53 – 7.50 (m, 2H), 7.48 – 7.45 (m, 2H), 7.25 (dd, 1H, *J* = 8.2, 0.8 Hz), 7.17 (d, 2H, *J* = 8.4 Hz), 7.15 (s, 1H), 7.10 (d, 2H,*J* = 8.4 Hz), 5.55 (s, 2H), 5.50 (s, 2H), 5.50 (s, 2H), 5.38 (s, 2H). HRMS (ESI+): *m/z* $(M+H)^+$ intended for $C_{30}H_{23}Br_2N_7O_3$ 690.02747, found as 690.02733.

1-(4-methoxybenzyl)-1H-1,2,3-triazol-4-yl)methyl2-((1-(4-methoxybenzyl)-1H-1,2,3-triazol-4-yl)methoxy)quinoline-4-carboxylate (4.4)

A solution of azide 3.4(0.1 g, 0.61 mmol) and quinoline di acetylene 2(0.162 g, 0.62 mmol) in 1 mL of t-BuOH and 1 mL of water was treated with sodium salt of ascorbic acid ($C_6H_7O_6Na$) (60 × 10^{-3} g,

0.3 mmol). This was followed by addition of copper sulphate pentahydrate $CuSO_4.5H_2O$ (7.6 mmol, 0.03 mmol) at 25°C temperature and stirred for a duration of 8 h. The reaction mixture was evaporated and the solvent was removed. The remaining solid was diluted with 5 mL of water and extracted with 20 mL of EtOAc and organic layers were washed with 5 mL of brine and dried with sodium sulphate (Na_2SO_4). Then after evaporating the solvent the residue was purified using column chromatography (Silica gel: 60-120 mesh and 92% of ethyl acetate (EtOAc) in pet. Ether) to afford 4.4 (0.15 g, 42%) as a white solid; mp 157-160°C; IR ($CHCl_3$): 3204, 3164, 3084, 3092, 3028, 3020, 1804, 1540, 1644, 1372, 1300 cm^{-1}; ^1H NMR (500 MHz, $CDCl_3$): δ 8.22 (dd, 1H, *J* = 8.2, 1.4 Hz), 7.97 (d, 1H, *J* = 8.5 Hz),7.63 – 7.58 (m, 1H), 7.56 (s, 1H), 7.48 (s, 1H), 7.26 – 7.22 (m, 3H), 7.20 – 7.16 (m, 2H), 7.13 (s, 1H), 6.93 – 6.89 (m, 2H), 6.87 – 6.83 (m, 2H), 5.54 (s, 2H), 5.48 (s, 4H), 5.36 (s, 2H), 3.81 (s, 3H), 3.79 (s, 3H). HRMS (ESI+): *m/z* $(M+H)^+$ intended for $C_{32}H_{30}O_5N_7$ 592.2303, found as 592.2294.

1-(2-chlorobenzyl)-1H-1,2,3-triazol-4-yl)methyl2-((1-(2-chlorobenzyl)-1H-1,2,3-triazol-4-yl)methoxy)quinoline-4-carboxylate (4.5)

Though the preparation of 4.5 from 3.5 is similar to 4.4, the difference lies in purifying the residue through chromatographic column (Silica gel: 60-120 mesh and 94% of ethyl acetate in pet. Ether) to afford 4.5 (0.11 g, 44%) as a white solid; mp 157-160°C; IR ($CHCl_3$): 3140, 3076, 3007, 1777, 1728, 1651, 1588, 1561, 1444, 1229, 1151, 1046, 745. cm^{-1}; ^1H NMR (500 MHz, $CDCl_3$): δ 8.23 (dd, 1H, *J* = 8.2, 1.3 Hz), 7.97 (d, 1H, *J* = 8.5 Hz), 7.72 (s, 1H), 7.64 – 7.56 (m, 2H), 7.42 (ddd, 2H, *J* = 19.7, 7.9, 1.3 Hz), 7.36 – 7.20 (m, 6H), 7.17 – 7.12 (m, 2H), 5.69 (s, 2H), 5.58 (s, 2H), 5.56 (s, 2H), 5.51 (s, 2H). HRMS (ESI+): *m/z* $(M+H)^+$ calculated for $C_{30}H_{24}O_3N_7Cl_2$ 600.1312, found 600.130.

(1-(4-(benzyloxy)benzyl)-1H-1,2,3-triazol-4-yl)methyl2-((1-(4-(benzyloxy)benzyl)-1H-1,2,3-triazol-4-yl)methoxy)quinoline-4-carboxylate (4.6)

A solution of azide 3.6(92 mg, 0.376 mmol) and quinoline di acetylene 2 (100 mg, 0.376 mmol) taken in a mixture containing 1 mL of t-BuOH and 1 mL of water was treated with sodium salt of ascorbic acid ($C_6H_7O_6Na$) (37 × 10^{-3} g, 0.188 mmol). This was followed by addition of copper sulphate pentahydrate (4.7 × 10^{-3} g, 0.018 mmol) at 25°C temperature and stirred for a duration of 8 h. The reaction mixture was evaporated to remove the solvent. The remaining residue was diluted with 5 mL of water and extracted with 20 mL of ethyl acetate and organic layers were washed with 5 mL of brine and dried with sodium sulphate (Na_2SO_4). Then after evaporating the solvent the residue was purified using column chromatography (Silica gel: 60-120 mesh and 85% of ethyl acetate in pet. ether) to afford 4.6(0.12 g, 47%) as a white solid; mp 157-160°C; IR ($CHCl_3$): 3395, 3115, 3033, 2924, 1729, 1659, 1588, 1513, 1241, 771 cm^{-1}; ^1H NMR (500 MHz, $CDCl_3$): δ 8.22 (dd, 1H, *J* = 8.2, 1.3 Hz), 7.96 (d, 1H, *J* = 8.6 Hz, 1H), 7.60 (dd, 1H, *J* = 7.3, 1.3 Hz,), 7.57 (s, 1H), 7.64 – 7.53 (m, 1H), 7.49 (s, 1H), 7.45 – 7.28 (m, 10H), 7.24 (ddd, 3H, *J* = 8.4, 5.1, 2.3 Hz), 7.16 (d, 2H, *J* = 8.6 Hz), 7.14 (s, 1H), 7.00 – 6.94 (m, 2H), 6.94 – 6.89 (m, 2H), 5.53 (s, 2H), 5.47 (s, 2H), 5.47 (s, 2H), 5.35 (s, 2H), 5.05 (s, 2H), 5.03 (s, 2H).HRMS (ESI+): *m/z* $(M+H)^+$ calculated for $C_{44}H_{37}O_5N_7$ 744.2921, found 744.2928.

(1-(4-phenoxybenzyl)-1H-1,2,3-triazol-4-yl)methyl2-((1-(4-phenoxybenzyl)-1H-1,2,3-triazol-4-yl)methoxy)quinoline-4-carboxylate (4.7)

A solution of azide 3.7 (84 × 10^{-3} g, 0.376 mmol) and quinoline di acetylene 2 (100 × 10^{-3} g, 0.376 mmol) taken in a mixture containing 1 mL of t-BuOH and 1 mL of water was treated with sodium salt of ascorbic acid ($C_6H_7O_6Na$) (37 × 10^{-3} g, 0.188 mmol). Thiswas followed by addition of copper sulphate pentahydrate $CuSO_4$. (4.7 × 10^{-3} g, 0.018 mmol) at 25°C temperature and stirred for a duration of 8 h. The reaction mixture was evaporated to remove the solvent. The remaining residue was diluted with 5 mL of water and extracted with 20 mL of EtOAc and organic layers were washed with 5 mL of brine and dried with sodium sulphate (Na_2SO_4). Then after evaporating the solvent the residue was purified using column chromatography (Silica gel: 60-120 mesh and 95% EtOAc in pet. ether) to afford 4.7(0.13 g, 48%) as a white solid; mp 157-160°C; IR ($CHCl_3$): 3032, 2928, 1609, 1512, 1456, 1250, 1178, 1030, 763, 739 cm^{-1};^1H NMR (500 MHz, $CDCl_3$): δ 8.24 (dd, 1H, *J* = 8.2, 1.3 Hz), 7.96 (d, 1H,,*J* = 8.6 Hz), 7.64 (s, 1H), 7.63 – 7.58 (m, 1H), 7.55 (s, 1H), 7.36-7.23(m, 7H), 7.16 (s, 1H), 7.14 – 7.08 (m, 2H), 7.0-6.86 (m, 10H), 5.55 (s, 2H), 5.50 (s, 4H), 5.38 (s, 2H). HRMS (ESI+): *m/z* $(M+H)^+$ calculated for $C_{42}H_{34}O_5N_7$ 716.2616, found 716.2613.

(1-benzyl-1H-1,2,3-triazol-4-yl)methyl2-((1-benzyl-1H-1,2,3-triazol-4-l)methoxy) quinoline-4-carboxylate (4.8)

Though the preparation of 4.8 from 3.8 is similar to 4.7, the difference lies in purifying the residue

through chromatographic column (Silica gel: 60-120 mesh and 85% EtOAc in pet. Ether) to afford 4.8(90 mg g, 45%) as a white solid; mp 157-160°C; IR ($CHCl_3$): 3395, 3132, 3115, 3033, 2924, 2854, 1729, 1659, 513, 1242,1006, 771 cm^{-1}; ^1H NMR (500 MHz, $CDCl_3$): δ 8.22 (dd, 1H, *J* = 8.2, 1.3 Hz), 7.97 (d, 1H, *J* = 8.6 Hz), 7.64 – 7.58 (m, 2H), 7.52 (s, 1H), 7.42 – 7.27 (m, 8H), 7.25 – 7.19 (m, 3H), 7.14 (s, 1H), 5.55 (s, 4H), 5.49 (s, 2H), 5.43 (s, 2H). HRMS (ESI+): *m/z* $(M+H)^+$ calculated for $C_{30}H_{26}O_3N_7$ 532.2091, found 532.2089.

1-(2,4,6-trimethoxybenzyl)-1H-1,2,3-triazol-4-yl)methyl2-((1-(2,4,6-trimethoxybenzyl)-1H-1,2,3-triazol-4-yl)methoxy)quinoline-4-carboxylate (4.9)

Though the preparation of 4.9 from 3.9 is similar to 4.8, the difference lies in purifying the residue through chromatographic column (Silica gel: 60-120 mesh and and 95% EtOAc in pet. Ether) to afford 4.9 (0.11 g, 41%) as a white solid; mp 157-160°C; IR ($CHCl_3$): 3134, 3077, 2925, 2853, 1729, 1657, 1590, 1503, 1452, 1227, 1155, 1048, 756 cm^{-1};^1H NMR (500 MHz, $CDCl_3$): δ 8.25 (dd, 1H, *J* = 8.2, 1.4 Hz), 7.97 (d, 1H, *J* = 8.5 Hz), 7.64 (s, 1H), 7.60 (dd, 1H, *J* = 8.6, 1.4 Hz), 7.55 (s, 1H), 7.32 – 7.20 (m, 2H), 7.17 (s, 1H), 6.51 (s, 1H), 6.42 (s, 2H), 5.57 (s, 2H), 5.50 (s, 4H), 5.46 (s, 2H), 5.35 (s, 2H), 3.84 (s, 3H), 3.82 (s, 6H), 3.82 (s, 3H), 3.77 (s, 6H). HRMS (ESI+): *m/z* $(M+H)^+$ calculated for $C_{36}H_{38}O_9N_7$ 712.2725, found 712.2725.

(1-(4-fluorobenzyl)-1H-1,2,3-triazol-4-yl)methyl2-((1-(4-fluorobenzyl)-1H-1,2,3-triazol-4-yl)methoxy)quinoline-4-carboxylate (4.10)

A solution of azide 3.10 (57 mg g, 0.376 mmol) and quinoline di acetylene 2(100 × 10^{-3} g, 0.376 mmol taken in a mixture containing 1 mL of t-BuOH and 1 mL of water was treated with sodium salt of ascorbic acid ($C_6H_7O_6Na$) (37 × 10^{-3} g, 0.188 mmol) at 25°C temperature and stirred for a duration of 8 h. The reaction mixture was evaporated to remove the solvent. The remaining residue was diluted with 5 mL of water and extracted with 20 mL of ethyl acetate and organic layers were washed with 5 mL of brine and dried with sodium sulphate (Na_2SO_4). Then after evaporating the solvent the residue was purified using column chromatography (Silica gel: 60-120 mesh and 15% EtOAc in pet. ether) to afford 4.10 (0.1 g, 47%) as a white solid; mp 157-160°C; IR ($CHCl_3$): 3434, 3134, 3009, 1729, 1654, 1589, 1511, 1449, 1224, 1050 cm^{-1}; ^1H NMR (500 MHz, $CDCl_3$): δ 8.23 (dd, 1H, *J* = 8.2, 1.4 Hz), 7.97 (d, 1H,*J* = 8.5 Hz), 7.66 – 7.57(m, 2H), 7.52 (s, 1H), 7.33 – 7.27 (m, 2H), 7.26 – 7.19 (m, 3H), 7.14 (s, 1H), 7.11 – 6.99 (m, 4H), 5.54 (s, 2H), 5.52 (s, 2H), 5.49 (s, 2H), 5.40 (s, 2H). HRMS (ESI+): *m/z* $(M+H)^+$ calculated for $C_{30}H_{24}F_2N_7O_3$ 568.1892, found 568.1893.

Computations

Density functional theory (DFT) calculations[17-21] were conducted using Quantum chemical methods to evaluate the stability of bis 1,2,3-triazole derivatives of 2- Hydroxy quinoline-4-carboxylate. The Gaussian 09W program package[22-24] was employed for density functional calculations[25], while Gauss View 5.0.8[26] was utilised for visualization and preparation of input files. The binding affinity of these molecules to proteins was investigated through docking studies[17-21] utilising GOLD version 5.1[27]. Crystal structures retrieved from the Protein Data Bank (PDB) were imported into Accelrys Discovery Studio 2.1. The protein structures were then prepared for docking studies, using the clean protein protocol within Discovery Studio.

Density functional theory (DFT)

The results concerning all the eleven fully optimized molecular geometric structures of 2-Hydroxyquinoline-4-carboxylate derivatives in ground state are obtained using time dependent density functional theory (TD-DFT) with B3LYP functional and the 6-31G split basis set. Gaussview 5.0.8 is used to visualize frontier molecular orbitals and to study various quantum chemical properties.

The Chemdraw structures, ball and stick models, HOMO and LUMO molecular orbital energy diagrams, UV and IR spectrum are displayed in (Fig. 1) for 2 and 4.1. The information regarding the reactivity and selectivity of the compounds for all the synthesized molecules2, 4.1-4.10 listed in (Table 2) is presented through computational data. The data includes the calculated DFT values such as single point energy, HOMO, LUMO, ΔE (E_{LUMO}-E_{HOMO}) representing the energy gap, Chemical Potential (μ), Dipole Moment D, UV-Visible absorption maxima along with oscillator strength and log P. The data pertains to the optimised molecular structures of the synthesized molecules 2 and 4.1-4.10 in their ground state and it has been included in (Table 2).

The highly negative minimum energy values E_{min} suggests that the molecules are extremely stable. The molecular interacting ability is determined from HOMO-

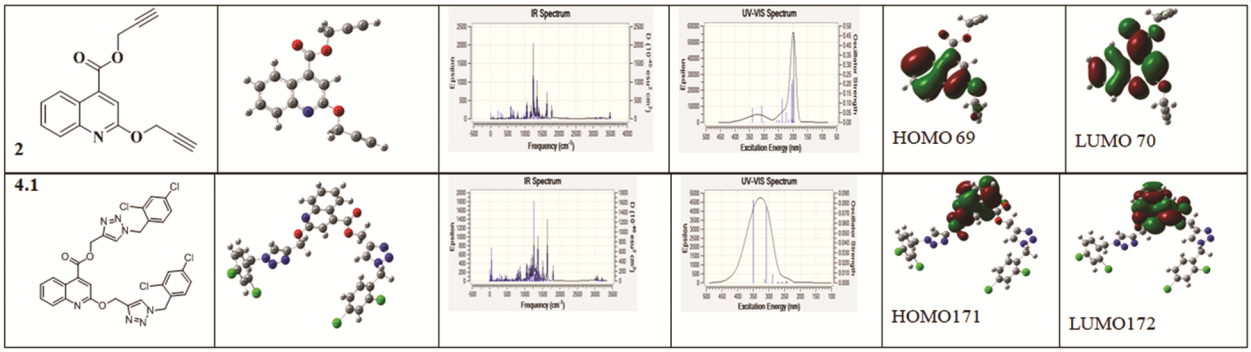

Fig. 1 — Display of chemdraw structures, Ball and stick models, UV and IR spectrum and Molecular orbital energy diagrams HOMO and LUMO of Compound 2,4.1 from DFT calculations

Table 2 — Calculated DFT data Energy, HOMO, LUMO, ΔE, Chemical Potential (μ), Dipole Moment D, UV-Vis absorption maxima (oscillator strength), and Log P of Optimised Molecules 2, (4.1-4.10)

Name	2	4.1	4.2	4.3	4.4	4.5	4.6	4.7	4.8	4.9	4.10
Energy (a.u)	-896.00	-3605.49	-3605.49	-3909.03	-1996.17	-2659.85	-2429.47	-2351.84	-1746	-2425.9	1953.08
HOMO (a.u)	-0.3313	-0.3734	-0.32289	-0.3243	-0.3074	-0.3223	-0.3094	-0.30902	-0.32162	-0.3155	-0.3244
LUMO (a.u)	0.0514	0.0576	0.05089	0.0464	0.0489	0.0529	0.05082	0.04762	0.04968	0.0529	0.0398
ΔE(a.u) = E_{LUMO}-E_{HOMO}	0.3826	0.4310	0.37378	0.3707	0.3074	0.3753	0.3094	0.30902	0.3216	0.3155	0.3643
μ (a.u) = (E_{LUMO}+E_{HOMO})/2	-0.13995	-0.1579	-0.136	-0.13895	-0.1292	-0.1347	-0.1292	-0.1307	-0.1359	-0.1312	-0.1423
Dipole Moment D	0.526	6.1584	8.8375	2.9952	8.0779	2.287	8.6707	8.8964	3.360	2.5789	4.83
UV-Vis nm											
n → π*	~340 (0.08)	349.22 (0.083)	349.40 (0.087)	349.06 (0.087)	349.78 (0.09)	238.43 (0.11)	325 (0.042)	240 (0.11)	320 (0.08)	350 (0.085)	240 (0.15)
π → π*	200 (0.45)	308.27 (0.017)	238.16 (0.16)	238.51 (0.17)	239.76 (0.10)			200 (0.09)		240 (0.19)	185 (0.02)
Log P	0.7	0.26	0.26	1.26	-0.83	0.71	2.72	2.53	1.15	-4.8	-0.05

LUMO frontier orbital gap not only explains stability but also reflects on chemical reactivity of the molecule.

All the eleven inhibitors synthesized are highly stable HOMO energy of ~ -0.3 a.u (8.163 eV) and LUMO energies ofthe order of~ 0.05 au (1.3606 eV). This results in ΔE as~ 0.35 a.u (9.5 eV). The molecular orbital energy diagrams show highly localized charge density distribution on the quinoline moiety. This states that the substituted quinoline moiety can be used for the design of drug molecules.

Large dipole moment values ranging between 2.3 D to 8.83 D indicate the polar nature of the molecules. The high dipole moment values can lead to the directional orientation of molecules in space making them more water soluble. The ligands with low dipole moment (~ 2 D) are more lipophilic, indicating drug like behaviour than those with high dipole moment values (~ 8D).

The chemical potential μ is associated with the tendency of molecular system to exchange electron density in its ground state. Negative of chemical potential μ is Mulliken electronegativity χ = - μ. The increase in chemical potential μ, *i.e.*, the tendency to exchange electron density of the synthesized derivatives leads to decrease in electronegativity χ (= - μ) of the substituent. In any chemical process, the systems evolve towards criteria of minimum energy. The highly negative energies make the molecules very stable. The DFT calculations data in Table 2 states that the synthesized molecules may possess good biological activity.

TD-DFT calculations predict two broad electronic transitions π → π* around 200 nm (oscillator strength f = 0.5) and n → π* around 300 nm (oscillator strength f =0.1757) and are in very good agreement with UV spectral data as listed in (Table 2).

Infrared (IR) analysis

To ascertain the accuracy of the chosen level of theory, a comparison was made between the experimental vibrational frequencies and the computed vibrational wave numbers, taking into account their corresponding IR intensities and normal modes of vibration. Table 3 presents the theoretically calculated vibrational wave numbers for the compounds.

A strong band around 1644–1788 cm^{-1} in quinoline 4-carboxylate derivatives shows the presence of C=O group. The strong band in FTIR spectra around 1644 cm^{-1} is due to C=O stretching vibrations while the calculated value for monomer is at 1793 cm^{-1}, and the value in case of dimer is close to the experimental value.

The intense band (exp.: 1727 cm^{-1}) is due to the carbonyl vibration. In the molecules the ν_{NH} stretching frequency is at 3204 cm^{-1}. Based on the degree of hydrogen bonding there can be variation in the band stretch from 3500-3200 cm^{-1} region. A sharp peak at 1644-1788 cm^{-1} is assigned to $\nu_{C=O}$. The vibrational frequency ν_{C-O} is observed around 1252-1364 cm^{-1}. A broad band of peaks observed ranging from 1200 to 1300 cm^{-1} may be due to the merge of ν_{C-O} and $\nu_{C=N}$ in the molecule. In the ring, $\nu_{C=N}$ vibrational frequency is observed at 1350-1390 cm^{-1} and $\nu_{N=N}$ stretching frequency is noted around 1500 cm^{-1}.

A study of all the spectra of molecules, revealed major changes in stretching frequencies of free C=N, ring C=N, N-N and C=O vibrations. The C-X stretch vibration peak is observed at 742 cm^{-1} support the lack of involvement of imino nitrogen atom on coordination. The strong broad band observed in the region 3600-2500 cm^{-1} can be due to ν_{O-H} and ν_{N-H} stretching frequencies. The rocking and wagging modes are observed in the range of 825-904 cm^{-1} and 617-638 cm^{-1}.

Comparison of computed wave numbers with experimental values reveal an overestimation of the vibrational wave numbers due to neglect of the anharmonicity present in the actual system. The IR frequencies obtained have 10% deviation from standard absorption frequencies.

The computed vibrational wave numbers, their intensities, carried out with DFT using Gaussian 09 program are compared with that of IR experimental data and are found to be in good agreement.

Biological evaluation

In vitro antitubercular and antimicrobial studies were conducted on the synthesized quinoline derivatives using *M. bovis* (BCG) a surrogate model for antimycobacterial activity and zone of inhibition method for antibacterial activity and antifungal activity.

Antimycobacterial assay

M. bovis (BCG) is a surrogate model to screen chemicals and identify new antimycobacterial agent. Initially, a single concentration (30 μM) of each compound was screened against BCG in 96-well flat-bottom polystyrene microtiter sterile plates

Table 3 — Few Selective Theoretical IR vibrational frequencies in cm^{-1} of ligands

S. No	Compound No.	ν_{N-H}	$\nu_{C=O}$	$\nu_{C=C}$	ν_{C-N} (free)	$\nu_{N=N}$	ν_{C-O}	others
1	2	3204	1788	1648	1357	1516	1248; 1048	ν2494, 2495 (aliphatic C (triple bond) C stretch) ν 3219 (aromatic stretch)
2	4.1	3204	1788	1644, 1804	1308, 1372	1516, 1548	1252, 1260	ν_{C-Cl}868,1068
3	4.2	3204-3220	1644	1636, 1796	1364	1516	1260, 1268	ν_{C-Cl}804,956
4	4.3	3204	1644	1644, 1804	1460	1510, 1540	1260, 1364	ν_{C-Br} 1060,1180
5	4.4	3020, 3028	1777, 1728	1804	1644	1540	1300, 1372	υ_{O-CH3} 1060,796
6	4.5	3140,3076	1788		1651	1588, 1544	1229, 1151	ν_{C-Cl}780
7	4.6		1805	1644, 1804	1316	1516, 1548	1268, 1385	ν_{C-H} 3076,3056 (aliphatic stretch) 3192 (aromatic stretch)
8	4.7		1759	1642	1312$\nu_{C=N}$ 1642	1516, 1548	1114, 1259	ν_{C-H} 3227 (aromatic stretch)
9	4.8	3334, 3343	1804		1399	1561	1282	ν_{C-H}3208 (aromatic stretch) 670,688,760,1039 1075,1102,1201
10	4.9		1861	1601, 1662	1294		1373	ν_{C-H}3203 (aromatic stretch) in OCH_3 3037.44,3056.88
11	4.10	3204		1747	1308, 1372	1449	1380,1156, 1142	ν_{C-F} 1346,1335

(Nunc). Dilutions of all compounds were prepared in DMSO. The activity of the synthesised molecules, was evaluated in comparison to positive controls *viz*., Rifampicin and Isoniazid, as well as solvent controls such as DMSO, media control (blank), which were included to inhibit BCG growth in each plate.

In each assay plate, one column was dedicated to the negative control DMSO representing 100% growth, while another column contained the positive controls (Rifampicin and Isoniazid). These controls served to monitor the quality of the assay and normalize the data on a per-plate basis. The growth inhibition effect of synthesised compounds was calculated using the standard expression:

$$\% \text{ Inhibition} = 100\ [OD_{\text{with compound}} - OD_{\text{of Negative control}}] / [OD_{\text{of Positive control}} - OD_{\text{of Negative control}}]$$

$$\% \text{ Inhibition} = [(A_{control} - A_{sample})\_/A_{control}]\_ \times 100$$

where $A_{control}$ is the absorbance of the control, A_{sample} is the absorbance of the test compounds. All the compounds synthesized were found insensitive towards mycobacterial strains (Table 4).

Antimicrobial activity

The well plate method was employed to assess the antibacterial and antifungal activities of the synthesised compounds against pathogenic microorganisms by measuring the zone of inhibition. The two gram positive bacteria *viz*., *Staphylococcus aureus (MTCC3 160), Bacillus subtilis (MTCC736)*, the three gram negative bacteria *viz*., (*Klebsiella pneumonia (MTCC 39), Salmonella typhi* (98), *Escherichia coli* (40) and fungal *Candida albicans (MTCC1637)* strains were used to study antimicrobial activity. All the synthesised triazole derivatives of 2-hydroxyquinoline-4-carboxylate showed increasing antibacterial activity towards the tested cultures. A good inhibition value of ~25 mm was observed for 2 and 4.6 against *Staphylococcus aureus*, for *Bacillus subtilis* and gram negative bacteria such as *Klebsiella pneumonia*, *Escherichia coli*, *Salmonella typhi* and *B. subtilis*, whereas, an activity of 18 to 24 mm was observed for other derivatives. The antifungal activity of synthesized derivatives were tested against *C. albicans*. Of all the compounds 2 and 4.6 showed good activity of 25 mm against the tested fungal strain.

Table 4 — Mycobacterial activity of derivatives of 2- Hydroxyquinoline-4-carboxylate

S. No.	1	2	3	4	5	6	7	8	9	10	11
Sample code	2	4.1	4.2	4.3	4.4	4.5	4.6	4.7	4.8	4.9	4.10
% of Inhibition	-30.35	-3.22	13.48	-12.66	7.75	-21.75	0.57	-15.02	-8.19	-12.96	-5.63

Table 5 — Antibacterial activity of bis 1,2,3-triazole derivatives of 2-Hydroxyquinoline-4-carboxylate (2 and 4.1-4.10) compounds

		Anti-bacterial activity, Zone of inhibition in millimetres Conc.100 µL/one well					Anti-Fungal Activity Zone of inhibition in millimetres (mm) Conc.100 µL/one well
S. No	Compound No.	Gram-positive		Gram-negative			Fungi
		S. aureus	*B. subtilis*	*K. pneumoniae*	*E. coli*	*S. Tiphi*	*C. albicans*
1	2	25	20	25	25	25	25
2	4.1	20	22	22	20	20	22
3	4.2	20	22	22	22	22	22
4	4.3	20	22	22	20	22	22
5	4.4	19	20	20	20	20	20
6	4.5	21	20	20	22	22	20
7	4.6	24	25	25	24	25	25
8	4.7	20	20	20	20	20	20
9	4.8	20	20	20	24	20	20
10	4.9	18	20	20	20	20	20
11	4.10	18	18	19	20	20	19
	Standard	30	30	30	28	33	28

Standard: Streptomycin in DMSO for Gram-positive and Gram-negative bacteria — Standard Fluconazole

Molecular docking studies

Molecular Docking study of the optimized 2-Hydroxyquinoline-4-carboxylicacidtriazole derivatives was done to evaluate their affinity at the active site of (1) DNA gyrase B protein of *Staphylococcus aureus* a Gram positive bacterium, (2) DHFR of *Candida albicans* fungi, and (3) InhA protein of *Mycobacterium tuberculosis*.

The binding affinity in this study is quantified using the GOLD score. The default GOLD fitness function and parameters were used to generate the optimal conformations for both the ligand and the protein. The Gold score is computed based on a molecular mechanics-based function specifically designed to optimize the binding positions of the ligand within the receptor's binding pocket. It takes into account various factors, including hydrogen bonding interactions between the protein and ligand ($S_{hb\text{-}ext}$), van der waals interactions between the protein and ligand ($S_{vdw\text{-}ext}$), hydrophobic interactions within the ligand ($S_{hb\text{-}int}$), and contributions from intramolecular strain experienced by the ligand (S_{int}), which includes $S_{vdw\text{-}int}$ and S_{tors}, representing torsional strain.

$$\text{Fitness} = S_{hb\text{-}ext} + 1.3750 \times S_{vdw\text{-}ext} + S_{hb\text{-}int} + 1.000 \times S_{int}$$

and $S_{int} = S_{vdw\text{-}ext)} + S_{(tors)}$

Docking study with DNA Gyrase b protein of *Staphylococcus aureus*

Quinolines exert their inhibitory effect on DNA synthesis by inducing the cleavage of bacterial DNA gyrase and type-IV topoisomerase which causes rapid demise of bacteria. To get better insight into the structural aspects of the synthesised molecules 2, (4.1-4.10) molecular docking study was performed against DNA gyrase of *Staphylococcus aureus*, a Gram positive bacterium. The GOLD docking summary of the best poses with suitable binding and with crucial interactions of the residues in the active site are tabulated in Table 6.The stability of the ligand in its best docked pose is determined by the hydrogen bonding interactions with the amino acids in the protein. Among them, molecule 4.6 exhibited the highest fitness score of 58.20, indicating a strong binding affinity and favourable hydrogen bond interactions. The molecule 4.6 bonding with amino acid residues of Gyrase B (PDB ID: 3G75) is shown in (Fig. 2).

The 4.6 with fitness score 58.20 formed three important hydrogen bonds with active site pocket residues of protein DNA Gyrase B (3G75). The first Hydrogen bond is between the NH of Asp81 with O13 atom of 4.6 with a Hydrogen bond distance of 3.387 Å, and other two hydrogen bonds formed with Ile86, one with Hydrogen bond distance 3.041

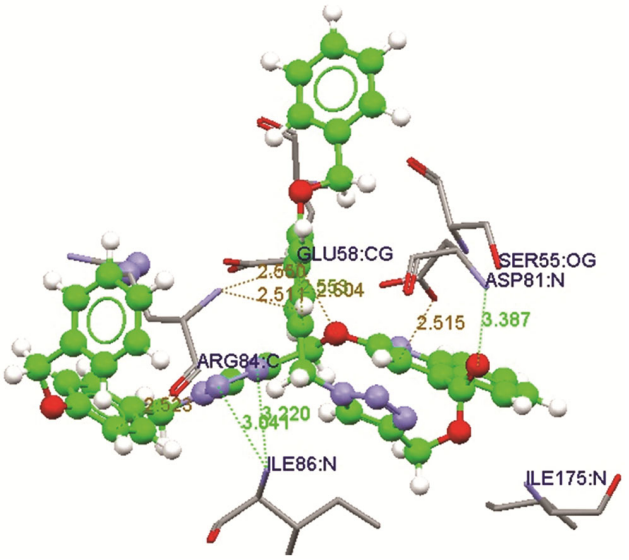

Fig. 2 — Hydrogen bond interactions of Compound 4.6 and *Staphylococcus aureus, DNA* Gyrase B (PDB ID: 3G75 resolution 2.3 Å). The hydrogen bonding interactions are represented with green dotted lines and amino acids as stick models

Table 6 — GOLD Scores of 2, (4.1-4.10) compounds with *Staphylococcus aureus* Gyrase B (3G75)

Ligand Name	$S_{hb\text{-}ext}$	$S_{vdw\text{-}ext}$	$S_{hb\text{-}int}$	S_{int}	Fitness Score
2	1.38	24.93	0.00	-4.48	31.17
4.1	1.65	48.73	0.00	-15.48	53.17
4.2	3.71	43.87	0.00	-13.24	50.81
4.3	4.59	43.00	0.00	-9.08	54.64
4.4	1.92	43.88	0.00	-7.89	54.37
4.5	3.74	45.62	0.00	-12.37	54.10
4.6	2.33	49.95	0.00	-12.81	58.20
4.7	1.27	53.78	0.00	-20.24	54.98
4.8	1.55	43.69	0.00	-7.94	53.67
4.9	2.48	45.90	0.00	-23.19	42.40
4.10	1.22	45.77	0.00	-11.09	53.07

Å (Ile86: NH----N19), and other with Hydrogen bond distance 3.220 Å (Ile86: NH----N20). And, other close interactions are seen in (Fig. 2) with the amino acids Ser55, Arg84, Ile86, Glu58, Asp81 and Ile175.

Docking studies of compounds with DHFR of *Candida albicans*

The crystal structure of *Candida albicans* DHFR with a resolution of 1.71 Å is extracted from the PDB database (PDB ID: IM78).

Molecular docking studies of synthesized compounds 2, (4.1-4.10) along with the protein receptors was carried out to find the binding affinities and significant interactions between the DHFR of *Candida albicans* and synthetic derivatives using GOLD (Table 7).

Compound 4.6 showed reasonable activity with protein IM78 active site (Fig 3). It showed good docking score of 71.97, and has good binding pattern within the active site. Ala11, Tyr113, Phe36 and Tyr118 of the protein showed hydrogen bonding interactions with the compound and the strong hydrogen bond between Ala11: N------O14 of the Compound with distance 2.265 Å is observed residues Phe36, Ile112, Met25 ,Gly114, Ile9 and Ala115 are stabilised through hydrophobic interactions.

Subsequently, using fitness score of 2-Hydroxyquinoline-4-carboxylic acid derivatives from (Table 7), the potent antimicrobial agents were explored and are compared with experimental antimicrobial data.

The docking score of DNA gyrase B protein of *Staphylococcus aureus* and DHFR of *Candida albicans* are mentioned for brevity in (Table 8).

Docking studies with MTB INHA

To assess the structure activity relationships of these (2 and 4.1-4.10) compounds a preliminary docking study is carried out using GOLD software version 5.1. Docking score is obtained by comparing these molecules with a reference *viz*., acyclic 4R isomer of INH-NADP a derivative of the prodrug Isoniazid which inhibits the protein (PDB ID: 2CIG protein used for docking) of *Mycobacterium tuberculosis*. The reference compound showed a docking score of 155.41. Compared to the reference compound, out of the 11 compounds studied, five compounds showed less than 60% docking score as mentioned in (Table 2) and *in vitro* studies revealed no activity with M. tb strains. A comparative analysis of theoretical docking score with that of the

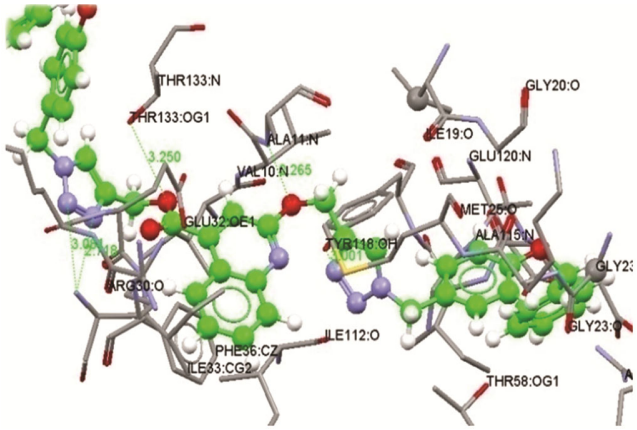

Fig. 3 — Binding orientationof compound 4.6 in DHFR of *C. albicans* active site

Table 7 — GOLD Scores of 2, (4.1-4.10) compounds with DHFR of *Candida albicans* B (3G75)

Ligand Name	$S_{hb\text{-}ext}$	$S_{vdw\text{-}ext}$	$S_{hb\text{-}int}$	S_{int}	Fitness score
2	1.66	36.00	0.00	-5.97	45.19
4.1	4.16	61.69	0.00	-14.67	74.31
4.2	0.95	66.28	0.00	-14.51	77.57
4.3	1.15	62.18	0.00	-10.34	76.31
4.4	2.05	58.84	0.00	-18.94	64.01
4.5	1.23	57.54	0.00	-6.71	73.64
4.6	2.69	73.31	0.00	-31.53	71.97
4.7	0.97	69.82	0.00	-22.54	74.44
4.8	1.54	58.14	0.00	-16.36	65.12
4.9	2.68	59.37	0.00	-23.04	61.28
4.10	3.01	58.56	0.00	-17.80	65.73

Table 8 — GOLD Docking Results of (A) DNA gyrase B protein of *Staphylococcus aureus*, (B) DHFR of *Candida albicans*

	2	4.1	4.2	4.3	4.4	4.5	4.6	4.7	4.8	4.9	4.10
A	31.17	53.17	50.81	54.64	54.37	54.10	58.20	54.98	53.67	42.40	53.07
B	45.19	74.31	77.57	76.31	64.01	73.64	71.97	74.44	65.12	61.28	65.73

Table 9 — GOLD Docking Scores of MTb-InhA protein of Reference compound R and 2, 4.1-4.10 the synthesized triazole derivatives of 2- hydroxy quinoline-4-carboxylic acid

R	2	4.1	4.2	4.3	4.4	4.5	4.6	4.7	4.8	4.9	4.10
155.41	30.45	95.95	92.76	93.37	92.45	95.83	83.45	62.12	95.83	89.12	80.12

experimental % of inhibition to *M. bovis* indicates that a better activity may be possible with proper designing of ligand molecules (Table 9).

Conclusion

The novel bis 1,2,3-triazole derivatives of 2-Hydroxyquinoline-4-carboxylate (2, 4.1-4.10) were synthesized using click reaction. This paper focuses on the synthesis, biological evaluation and structural investigation of these molecules, both experimentally with NMR, HRMS, IR techniques and theoretically using DFT calculations and docking studies.

DFT calculations demonstrated the stability of all synthesized molecules. The dipole moments, absorption wavelength, log p values and other theoretical parameters are comparable with experimental data.

Molecular docking study conducted on the optimized 2-Hydroxyquinoline-4-carboxylate derivatives with (1) DNA gyrase B protein (PDB ID: 3G75) of *Staphylococcus aureus* (Gram positive bacterium); (2) DHFR protein (PDB ID: IM78) of *Candida albicans;* and (3) Mtb Inha Protein (PDB ID: 2CIG) was aimed to investigate the interaction of the synthesised derivatives with the respective target proteins. The protein ligand stability towards DNA gyrase of *Staphylococcus aureus* and DHFR of *Candida albicans* is influenced by hydrogen bond interactions between critical amino acids present in the protein and ligand. The synthesized compounds exhibited favourable docking scores with DNA gyrase of *Staphylococcus aureus*, DHFR of *Candida albicans,* suggesting their potential for the development of new bacterial and fungal drugs. Regarding the docking studies of the ligands with InhA protein, it was observed that the hydrophobic interactions were maintained. However, a decrease in hydrogen bonding interactions and cation–pi interactions led to a reduction in stabilizing interactions in the protein-ligand complex.

The observed percentage of Inhibition of tubercular activity for these compounds may be due to the inadequate presence of hydrogen-bonded interactions and the shift of the hydrophobic pocket within the protein ligand complex. The increased mass of ligand and the presence of electro negative atoms within the hydrophobic pocket could weaken the stabilizing interactions, despite the molecules being polar. Additionally, the reduced flexibility of the ligand in the binding pocket, resulting from its structural symmetry could also contribute to the decrease in activity. These factors likely resulted in lower experimental and theoretical score values.

All the synthesised derivatives exhibited significant antimicrobial activity against two-gram positive bacteria *Staphylococcus aureus (MTCC3160), Bacillus subtilis (MTCC736)*, as well as gram negative bacteria (*Klebsiella pneumonia (MTCC 39), Salmonella typhi (98), Escherichia coli (40)* and *Candida albicans (MTCC 1637)*.

The insights gained from the docking scores with InhA and Mtb *in vitro* activity suggest that, prospective lead compounds based on quinoline derivatives can be designed to enhance the structure activity relationship for anti-tubercular activity. Therefore, proper molecule design aimed at achieving the desired hydrogen bonding, cation–pi and pi-pi interactions and flexibility of the ligand within the binding pocket can promote favourable docking scores and *in vitro* Mtb activity.

The DFT calculations and docking score data of the synthesized compounds were consistent with the experimentally observed values. Therefore, we conclude that, these molecules hold promise for further exploration and development as antibacterial and antifungal agents.

Acknowledgement

One of the authors, Mrs. K Usha Rani, is thankful to UGC-SERO, for awarding teacher fellowship under FDP, to CSIR-IICT Hyderabad, for giving opportunity to carry out synthesis work and to School of Chemistry, University of Hyderabad for permitting her to pursue computational work through UGC-NET Working centre.

Conflict of interest

All authors declare no conflict of interest.

References

1 Vatmurge NS, Hazra BG, Pore VS, Shirazi F, Chavan PS & Deshpande MV, Synthesis and antimicrobial activity of beta-lactam-bile acid conjugates linked *via* triazole. *Bioorg Med Chem Lett,* 102 (2008) 2043.

2 Agalave SG, Maujan SR & Pore VS, Click Chemistry: 1,2,3-Triazoles as Pharmacophores. *Chem Asian J*, 6 (2011) 2696.

3 Holla BS, Gonsalves R & Shenoy S, Studies on some N-bridged heterocycles derived from bis -[4-amino-5-mercapto-1,2,4-triazol-3-yl] alkanes. *Farmaco* 53 (1998) 574.

4 Masuda K, Toga T & Hayashi, N, Synthesis of 3-morpholino-N-ethoxycarbonylsydnonimine-5-^{14}C(sin-10-^{14}C). *J Labelled Compd*, 11 (1975) 30.

5 Almasirad A, Tabatabai SA, Faizi M, Kebriaeezadeh A, Mehrabi N, Dalvandi A & Shafiee A, Synthesis and anticonvulsant activity of new2-substituted-5-[2-(2-

fluorophenoxy)phenyl]-1,3,4-oxadiazolesand 1,2,4.-triazoles. *Bioorg Med Chem Lett,* 14 (2004) 6057.

6 Holla BS, Poojary KN, Rao BS & Shivananda MK, New bis -aminomercaptotriazoles and bis -triazolothiadiazoles as possible anticancer agents. *Eur J Med Chem*, 37 (2002) 511.

7 Manclús JJ, Moreno MJ, Plana E & Montoya Á, Enzyme-Linked Immunosorbent Assay for the Quantitation of the Fungicide Tetraconazole in Fruits and Fruit Juices. *J Agric Food Chem,* 56 (2008) 8793.

8 Amir, M & Shikha, K, Synthesis and Anti-Inflammatory, Analgesic, Ulcerogenic and Lipid Peroxidation Activities of Some New 2-[(2, 6-Dichloroanilino) Phenyl]Acetic Acid Derivatives. *Eur J Med Chem,* 39 (2004) 535.

9 Mohammed Ali Hussaini Syed (2016): Therapeutic significance of quinolines: a patent review(2013-2015).

10 Senthilkumar P, Dinakaran M, Chandraseakaran Y, Perumal Yogeeswari & Sriram D, Synthesis and *in vitro* Antimycobacterial Evaluation of 1-(Cyclopropyl/2,4-difluorophenyl/tert-butyl)-1,4-dihydro -8-methyl-6-nitro-4-oxo-7-(substituted secondary amino) quinoline-3-carboxylicacids. *Arch Pharm Chem Life Sci,* 342 (2009) 100.

11 Dover LG & Coxon GD, Current status and research strategies in tuberculosis drug development. *J Med Chem,* 54 (2011) 6157.

12 Johnson JL, Hadad DJ, Boom WH, Daley CL, Peloquin CA, Eisenach KD, Jankus DD, Debanne SM, Charlebois ED, Maciel E, Palaci M & Dietze R, Early and extended early bactericidal activity of levofloxacin, gatifloxacin and moxifloxacin in pulmonary tuberculosis. *Int J Tuberc Lung Dis*, 10 (2006) 605.

13 A) Rajeev Kharb & Hardeep Kaur, Therapeutic significance of quinoline derivatives as antimicrobial agents. *Int Res J Pharm*, 4 (2013), and B) Dharshan JC, Vishnumurthy KAA, Bodke YD, Vagdevi HM, Jayanna ND & Raghavendra R, Synthesis, characterization and antimicrobial activity of 7-methoxy quinoline-4- substituted 1, 2, 3-triazole derivatives. *Der Pharma Chemica*, 4 (2012)272.

14 Kotapalli SS, Nallam SSA, Nadella L, Banerjee T, Rode HB, Mainkar PS & Ummanni R, Identification of new molecular entities (nmes) as potential leads against tuberculosis from open source compound repository. *PLoS One* 10 (2015) 12.

15 Rathod BB, Korasapati R, Sripadi P & Shetty PR, Novel actinomycin group compound from newly isolated *Streptomyces* sp. RAB12: isolation, characterization, and evaluation of antimicrobial potential. *Appl Microbiol Biotechnol,* 102 (2018) 1241.

16 Kandikonda S,Thesis on "The utility of organic azides and amine derivatives in medicinal chemistry" submitted to RMIT University, Aug 2015.

17 Çakmak Ş & Erdoğan T, Some bis (3-(4-nitrophenyl)acrylamide derivatives: Synthesis, characterization, DFT, antioxidant, antimicrobial properties, molecular docking and molecular dynamics simulation studies. *Indian J Biochem Biophys*, 60 (2023) 209.

18 Ramaswamy S, Kongara D, Priyanka DL, Gade R, Raj KR & Gayathri R, Synthesis, spectral characterization, antibacterial, cytotoxic evaluation and docking studies of new urea and thiourea derivatives. *Indian J Biochem Biophys*, 59 (2022) 767.

19 Erdogan T, Computational evaluation of 2-arylbenzofurans for their potential use against SARS-CoV-2: A DFT, molecular docking, molecular dynamics simulation study. *Indian J Biochem Biophys*, 59 (2022) 59.

20 Shahana FM & Yardily A, Synthesis, Quantification, DFT Calculation and Molecular Docking of (4-amino-2-(4-methoxyphenyl)aminothiazol-5yl)(thiophene-2-yl) methanone. *Indian J Biochem Biophys*, 57 (2020) 606.

21 Rani SM, Rose SV & Reji TFAF, Synthesis, characterization, dft calculation, docking studies, antioxidant and anticancer activities of some 3-(2-alkylaminothiazol-5-oyl)pyridines. *Indian J Biochem Biophys*, 57 (2020) 620.

22 Becke AD, Density-functional exchange-energy approximation with correct asymptotic behavior. *Phys Rev,* 38 (1988) 3098.

23 Becke AD, Density-functional thermochemistry. III. The role of exact exchange. *J Chem Phys,* 98 (1993) 5648.

24 Lee CT, Yang W & Parr RG, Development of the Colle-Salvetti correlation-energy formula into a functional of the electron density. *Phys Rev,* 37 (1988) 785.

25 Frisch MJ, Trucks GW, Schlegel HB, Scuseria GE, Robb MA, Cheeseman JR, Scalmani G, Barone V, Petersson GA, Nakatsuji H, Li X, Caricato M, Marenich A, Bloino J, Janesko BG, Gomperts R, Mennucci B, Hratchian HP, Ortiz JV, Izmaylov AF, Sonnenberg JL, Williams-Young D, Ding F, Lipparini F, Egidi F, Goings J, Peng B, Petrone A, Henderson T, Ranasinghe D, Zakrzewski VG, Gao J, Rega N, Zheng G, Liang W, Hada M, Ehara M, Toyota K, Fukuda R, Hasegawa J, Ishida M, Nakajima T, Honda Y, Kitao O, Nakai H, Vreven T, Throssell K, Jr. Montgomery JA, Peralta JE, Ogliaro F, Bearpark M, Heyd JJ, Brothers E, Kudin KN, Staroverov VN, Keith T, Kobayashi R, Normand J, Raghavachari K, Rendell A, Burant JC, Iyengar SS, Tomasi J, Cossi M, Millam JM, Klene M, Adamo C, Cammi R, Ochterski J W, Martin RL, Morokuma K, Farkas O, Foresman JB & Fox DJ, Gaussian, Inc., Wallingford CT, 2016.Gaussian 09.2013 Gaussian 09, Revision A.02, Gaussian, Inc., Wallingford CT.

26 Dennington R, Keith T & Millam J, *GaussView*, Version 5, *Semichem Inc., Shawnee Mission KS*, (2009).

27 Jones G, Willett P, Glen RC, Leach AR & Taylor R, Development and validation of a genetic algorithm for flexible docking. *J Mol Biol,* 267 (1997) 727.